Environmental Development 27 (2018) 47–57

Contents lists available at ScienceDirect

Environmental Development

journal homepage: www.elsevier.com/locate/envdev

Malaria incidences in South Africa linked to a climate mode in southwestern Indian Ocean

Swadhin K. Behera[a,*], Yushi Morioka[a], Takayoshi Ikeda[a], Takeshi Doi[a], Jayanthi V. Ratnam[a], Masami Nonaka[a], Ataru Tsuzuki[b], Chisato Imai[b], Yoonhee Kim[b], Masahiro Hashizume[b], Shingo Iwami[c], Philip Kruger[d], Rajendra Maharaj[e], Neville Sweijd[f], Noboru Minakawa[b]

[a] Application Laboratory, Japan Agency for Marine-Earth Science and Technology, Yokohama, Japan
[b] Institute of Tropical Medicine, Nagasaki University, Japan
[c] Department of Biology, Kyushu University, Japan
[d] Department of Health, Limpopo, South Africa
[e] Medical Research Council, Durban, South Africa
[f] Applied Center for Climate and Earth Systems Science, Cape Town, South Africa

ABSTRACT

Millions of individuals are at risk of malaria infection in sub-Saharan Africa. Compared to other highly affected countries on the continent, South Africa has an excellent record of malaria control. Nevertheless, the northeastern districts of the country, neighboring some of the worst malaria affected regions in southern Africa, still experience seasonal malaria outbreaks particularly during the summer months of September-February. The year to year variations of the malaria outbreaks in southern Africa, as in many other parts of the world, are often linked to interannual variations in rainfall and temperature. These meteorological factors in turn are seen to be associated with large-scale climate phenomena such as El Niño/La Niña. Here, we present evidence of a new mode of climate variation in the Indian Ocean that could explain the interannual variation of malaria incidences in South Africa. This phenomenon appeared as a dipolar association in the sea surface temperature (SST) anomalies of southwestern Indian Ocean. Both poles of the dipole strongly correlated with the malaria incidence index of Vhembe district, one of South Africa's highest malaria-affected districts. The identified correlations were stronger than those found with other climate phenomena such as El Niño/La Niña and Indian Ocean Dipole. A decadal shift in the SST dipole pattern was also observed, and the associated decrease in seasonal rainfall could partly explain the recent reduction in malaria cases.

1. Introduction

In South Africa, malaria is endemic in northeastern provinces of Limpopo, KwaZulu-Natal and Mpumalanga. The northeastern districts of Limpopo province (Fig. 1) neighboring Mozambique, Zimbabwe and Botswana are particularly affected and report a high number of cases annually (Maharaj et al., 2013; Raman et al., 2016). Malaria prevalence in these districts is distinctly seasonal with a large number of the cases reported during the warm and rainy months of September to February.

* Corresponding author.
E-mail address: behera@jamstec.go.jp (S.K. Behera).

https://doi.org/10.1016/j.envdev.2018.07.002
Received 31 January 2018; Received in revised form 29 June 2018; Accepted 3 July 2018
2211-4645/ © 2018 The Authors. Published by Elsevier B.V. This is an open access article under the CC BY-NC-ND license (http://creativecommons.org/licenses/BY-NC-ND/4.0/).

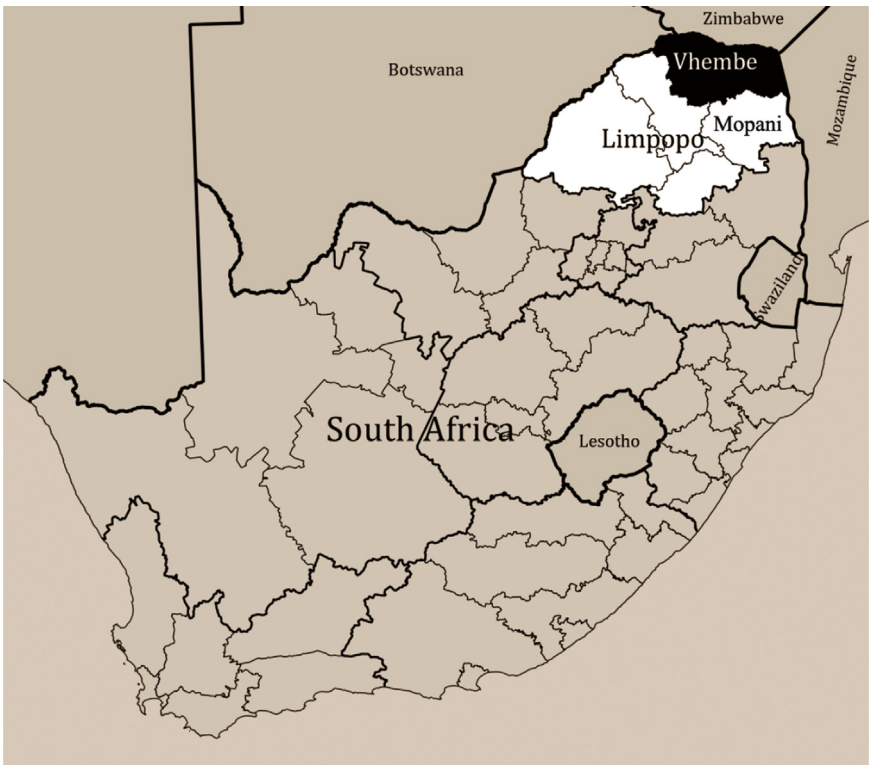

Fig. 1. The district of Vhembe in the study region of Limpopo province in South Africa.

Several studies have evaluated the impact of both climatic and non-climatic factors on the spatio-temporal distribution of malaria over southern Africa (Craig et al., 2004a; Jury and Kanemba, 2007; Mabaso et al., 2007; Moonasar et al., 2012; Maharaj et al., 2013; Raman et al., 2016). While discussing the variability of malaria incidence in South Africa, Craig et al. (2004b) suggested that the trends in malaria incidence could be affected by non-climatic factors such as the levels of drug/insecticide resistance, HIV prevalence and indoor residual spraying coverage among others. They reported that the non-climatic factors strongly affect the trend and variability in malaria transmission on the longer time-scales (several years to decades). They concluded that the transmission rate could be subjected to the effectiveness of control measures. In another recent study, however, Raman et al. (2016) found a rise in the number of malaria cases between 2012 and 2014 despite having a good control measure in South Africa. Therefore, understanding the relationship among climate factors, control methods and malaria transmission is important in developing an early warning system and improving the control measures.

Seasonal to interannual variations in malaria incidences have been reported to be associated with interannual climate phenomena, such as the El Niño/Southern Oscillation (ENSO). In general, below average malaria incidences are found during El Niño years and above average incidences are found during La Niña years (Mabaso et al., 2007). Since northeastern parts of South Africa are generally drier than normal during El Niño years, as compared to that in La Niña years, the number of cases of malaria transmission is expected to be lower than normal during those El Niño years. The Indian Ocean Dipole (IOD) is the other climate phenomena that significantly influence the regional rainfall patterns and malaria incidences particularly in the eastern side of the continent. Several studies have reported IOD's dominant influence on the malaria incidences in Kenya (Hashizume et al., 2009; Chaves et al., 2012; Hashizume et al., 2012). In addition, subtropical dipole phenomena in southern Atlantic and Indian Oceans have been shown to influence the climates of southern Africa (Behera and Yamagata, 2001; Reason, 2002; Fauchereau et al., 2003; Morioka et al., 2010). Therefore, we investigated the roles that these regional climate phenomena play in the interannual variability of malaria incidences in the Vhembe district, one of the highly-affected districts in South Africa. During the investigation, we identified a new climate phenomenon in the southwestern Indian Ocean that is significantly linked to the malaria incidences in the study region.

2. Data and methods

Malaria case data for Limpopo province including hospital records of patients are used in the analyses for the period 1998–2013. Data verification was done at the Tzaneen Malaria Institute in the Limpopo province and the details about the original data are discussed in Gerritsen et al. (2008). Further information about the monthly data used in this study are described in Ikeda et al. (2017). In brief, the digitized data were compiled monthly for each district, then monthly anomalies were computed by taking out the monthly climatology from the total monthly values as follows:

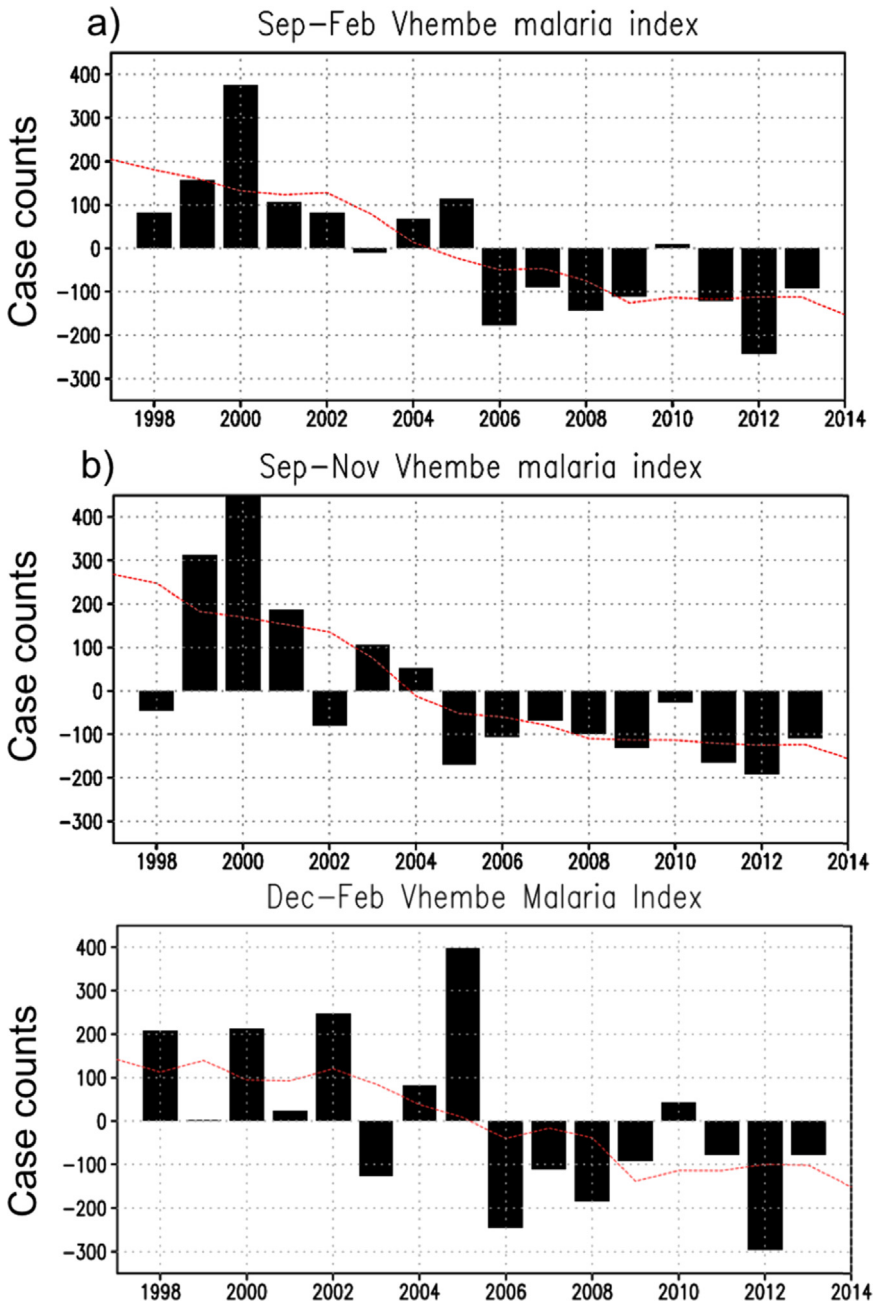

Fig. 2. Seasonal evolution of (a) VMI during September–February. A 7-year running mean of the index representing the decadal trend is shown as a dashed line. (b) and (c) are same as (a) but for September-November and December–February seasons, respectively.

$$M_i^{'} = Mi - \overline{M}$$

Where $M_i^{'}$ is the anomaly corresponding to each month "i", M_i is the monthly malaria counts and $\overline{M}$ is the monthly climatology obtained by averaging the monthly malaria counts for each month during the whole study period. The September-February averages of these monthly anomalies were then used to prepare the Vhembe malaria index (VMI) shown in Fig. 2. The VMI was correlated with climate data presented in Fig. 3–5, and Tables 1 and 2.

Vhembe – a northeastern district of the Limpopo province in South Africa (Fig. 1) has the highest reported malaria incidences in South Africa (Gerritsen et al., 2008; Maharaj et al., 2012; Raman et al., 2016). While there are other regions in the neighboring countries where the prevalence of malaria cases is substantially higher, accessing good quality archival of malaria case data from these regions, in order to establish robust statistical relations with climate data, is extremely challenging. As malaria case data from Vhembe were available from 1998, it was selected as the study area.

Table 1
Climate and VMI relationships at concurrent and 1-season lag. The first two rows show the correlation of Vhembe malaria index with the indices of EM_{SSTA}, SM_{SSTA}, Niño3, DMI and SDMI at lag 0 (concurrent for September-February) and lag 1 (September-February climate indices are correlated with June-November VMI), respectively. The last two rows show the corresponding correlations for EM_{SSTA}. Values above 0.47 are statistically significant at 95% using 2-tailed *t*-test.

	EM_{SSTA}	SM_{SSTA}	Nino3	DMI	IOSD
Vhembe (lag 0)	**− 0.73**	**0.58**	**− 0.25**	**− 0.41**	**0.1**
Vhembe (lag 1)	**− 0.79**	**− 0.48**	**− 0.35**	**− 0.55**	**− 0.16**
EM_{SSTA} (lag 0)	**1**	**− 0.62**	**0.55**	**0.19**	**0**
EM_{SSTA} (lag 1)	**0.82**	**− 0.61**	**0.51**	**0.30**	**0.15**

Table 2
Climate indices and VMI correlations after removing the linear trend from the data and the table is arranged same as Table 1.

	EM_{SSTA}	SM_{SSTA}	Nino3	DMI	IOSD
Vhembe (lag 0)	**− 0.63**	**0.62**	**− 0.25**	**− 0.38**	**0**
Vhembe (lag 1)	**− 0.73**	**0.53**	**− 0.35**	**− 0.54**	**− 0.20**
EM_{SSTA} (lag 0)	**1**	**− 0.61**	**0.63**	**0.16**	**0.12**
EM_{SSTA} (lag 1)	**0.68**	**− 0.59**	**0.61**	**0.27**	**0.20**

The seasonal progression of malaria incidence in Vhembe has a distinct annual cycle with malaria more prevalent during warm and humid months of September-February (Gerritsen et al., 2008; Maharaj et al., 2013; Ikeda et al., 2017). The reported incidences decrease drastically after May and remain low until August. Therefore, in this study we mostly focused on the months of September-February, which encompass spring and summer, when most cases are reported.

The climate data used here are the gridded SST anomalies derived from OISST (Reynolds et al., 2002) and 850 hPa winds derived from NCEP/NCAR reanalysis (Kanamitsu et al., 2002). Monthly-averaged SST data provided by Tokyo Climate Center (Ishii et al., 2005; JMA, 2006) were also used. The sea surface height (SSH) data were obtained from the NCEP-NCAR ocean reanalysis dataset. Precipitation anomalies were derived from Global Precipitation Climatology Center monthly precipitation gridded 0.5 × 0.5 degrees dataset (Schneider et al., 2013) based on global station data. The interannual monthly and seasonal anomalies for these climate fields were derived by removing monthly climatology from the total monthly values and then averaging for the September-February period. The base period chosen for making the monthly climatology was 1982–2013. The SST indices were then computed by taking area averages of SST anomalies over the domains as specified in the discussions.

3. Results and discussion

Seasonally averaged anomalies of malaria incidences showed clear interannual variations with highest and lowest incidences reported in 2000 and 2012, respectively (Fig. 2a). Case numbers vary slightly among years when the count period was separated into two seasons; September-November and December-February (Figs. 2b, 2c). For example, the lowest number of cases for both September-November (Fig. 2b) and December-February (Fig. 2c) seasons were found in 2012 as was the case for September-February averaged index (Fig. 2a). However, highest number of cases for December-February season was in 2005 (Fig. 2c) while the highest number of cases for the September-November season was in 2000 (Fig. 2b), as it was for the whole September-February period (Fig. 2a).

In addition to these year-to-year variations, a distinct phase-change in incidence rates was observed before and after 2006. Malaria incidences were above average prior to 2006 and below average (negative anomalies) thereafter, except for a near normal year in 2010 which was consistent with earlier reports (Gerritsen et al., 2008; Moonasar et al., 2012).

3.1. The climate link to interannual malaria incidences

The impact of interannual rainfall variations on malaria incidences in Vhembe was investigated by correlating the VMI with interannual anomalies of rainfall over the southern Africa (Fig. 3) during September-February. Significant positive correlations were seen over parts of Vhembe and Mopani (the district south of Vhembe, Fig. 1). Most importantly, significant correlation coefficients were also seen in parts of southern Mozambique and Zimbabwe. The rainfall anomalies in these neighboring countries appear to influence malaria transmission in Vhembe and other neighboring districts of Limpopo (e.g. Ikeda et al., 2017) through the cross-border transmission of the disease. The cause of the rainfall variability in that whole region associated with local and remote modes of climate variation would, therefore, be important to understand and predict the malaria incidences in Vhembe district. In this context, several previous studies had suggested that the summer rainfall anomalies in those regions are usually affected by the occurrences of El Niño/La Niña in the tropical Pacific (e.g. Kirtman et al., 2013; Christensen et al., 2013; Vigaud et al., 2009; Pohl et al., 2010). In general, the below-average rainfall years over much of southern Africa were associated with El Niño events (Mason, 2001; Giannini et al., 2008; Manatsa et al., 2008) though the local rainfall response could be varied (Fauchereau et al., 2009). On the contrary, La Niña events were associated with above normal rainfall over the region. Climate variability in adjacent southern Indian Ocean was

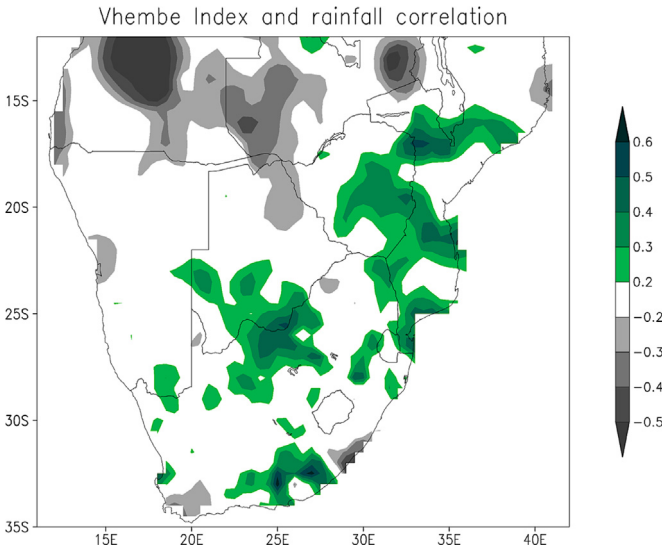

Fig. 3. The correlation of VMI with rainfall anomalies for September-February. Correlation values above 0.4 are statistically significant at 90% using a 2-tailed *t*-test.

also shown to influence the rainfall variability over southern Africa (Behera and Yamagata, 2001; Rouault et al., 2003; Hansingo and Reason, 2008, 2009; Hermes and Reason, 2008).

In order to examine a possible relationship between malaria incidences and basin scale climate variations, the VMI index was further correlated with the global anomalies of SST, sea level pressure (SLP) and surface wind. Interesting patterns of positive and negative correlation coefficients of SST anomalies were seen across southern Atlantic and Indian Oceans (Fig. 4). In particular, a meridional dipole pattern was prominent in southwestern Indian Ocean. This finding is analogous to several previous studies on the subtropical dipole pattern of the southern Indian Ocean (Behera and Yamagata, 2001; Reason, 2002; Morioka et al., 2010), however, the placement of the meridional dipole found in this study is different. The corresponding SLP correlation and wind regression maps revealed a connection to the subtropical high (Fig. 5) in the southern Indian Ocean with an anomalous anticyclone on top of the anomalous SST dipole pattern. The subtropical high, known as the Mascarene High, is a regular atmospheric feature in the southern Indian Ocean and its center is located to the eastern side of the subtropical southern Indian Ocean, nearer to Australian coast (Fig. 6). However, the western side of Mascarene High gets intensified during positive dipole years, when cold SST anomalies prevail east of Madagascar and warm SST anomalies prevail south of Madagascar (Fig. 4), shifting the center of the high westward (Fig. 5). This anomalous southwestward intensification of the Mascarene High would lead to higher moisture convergence and above normal rainfall (Fig. 3) over Vhembe and adjoining regions in Mozambique and Zimbabwe. These regions would experience an opposite

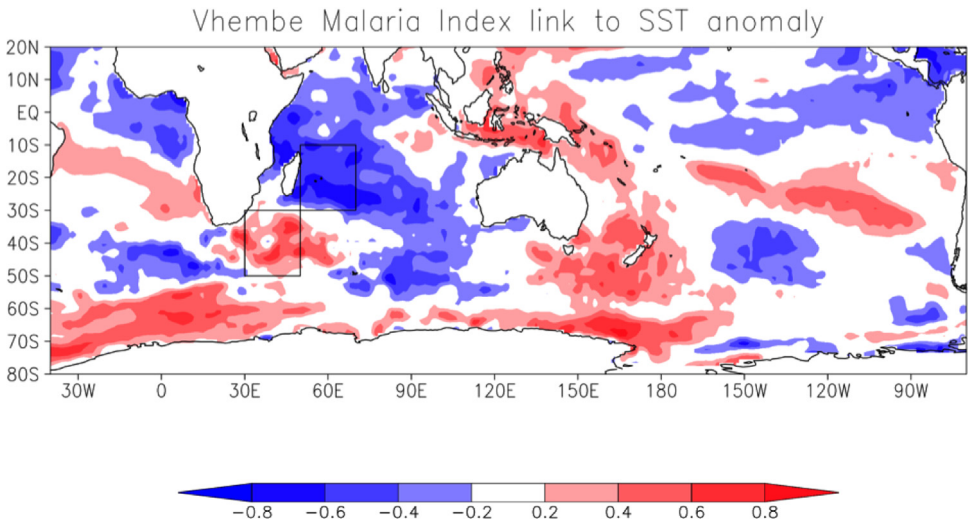

Fig. 4. The correlation of VMI with SST anomalies during September-February. Correlation values above 0.4 are statistically significant at 90% using a 2-tailed *t*-test. The boxes in the southwestern Indian Ocean are used to calculate EM_{SSTA} and SM_{SSTA}.

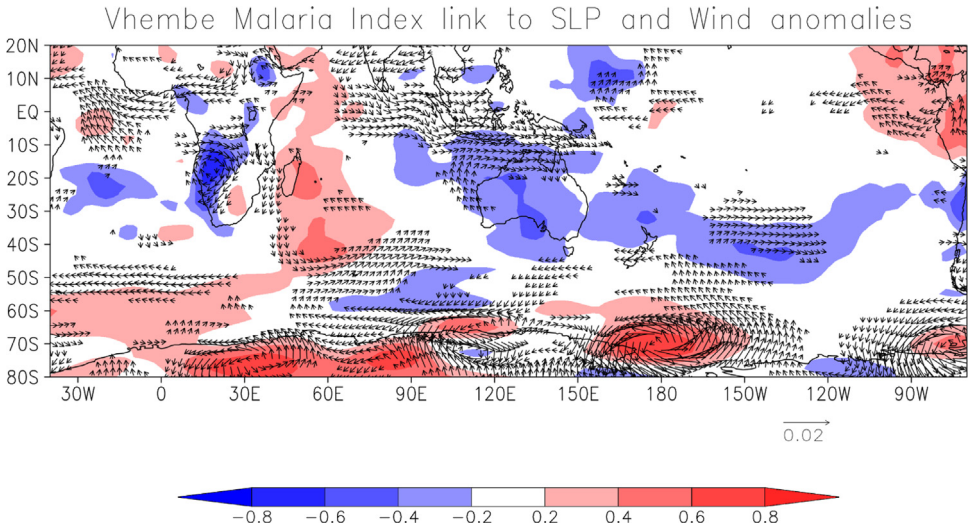

Fig. 5. The correlation of VMI with SLP anomalies and corresponding regression with 850-hPa wind anomalies during September–February. Correlation values above 0.4 are statistically significant at 90% using 2-tailed *t*-test.

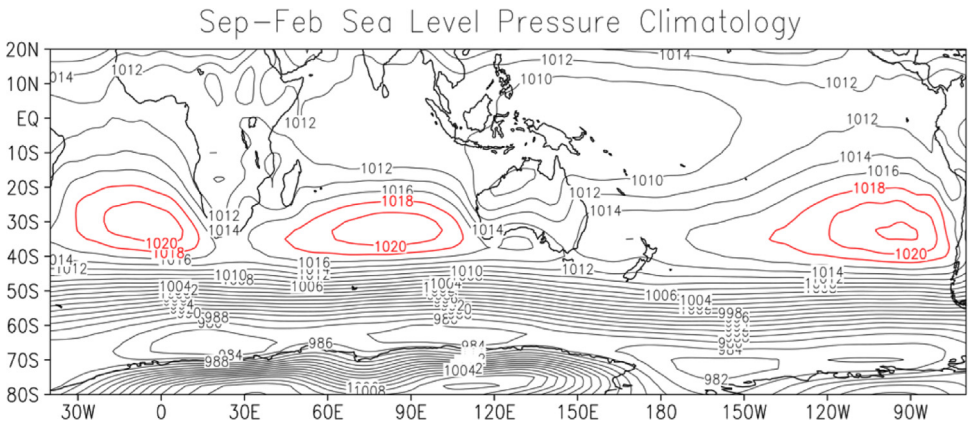

Fig. 6. Sea level pressure climatology for the September-February months. The core part of the Mascarene High (the Indian Ocean subtropical anticyclone) is highlighted in red contours together with the other two subtropical highs in Pacific and Atlantic Oceans (For interpretation of the references to color in this figure legend, the reader is referred to the web version of this article).

situation with below normal rainfall for a negative dipole year when warm SST anomalies prevail east of Madagascar and cold SST anomalies prevail south of Madagascar.

Interestingly, correlation patterns in the tropical Pacific and Indian Oceans suggest possible interactions with ENSO and IOD. The negative correlations in tropical Pacific are associated with higher malaria incidences during La Niña and vice versa. Also, a positive dipole pattern, seen with negative correlations in western tropical Indian Ocean and positive correlations on eastern tropical Indian Ocean (Fig. 4), suggests a connection of the positive Indian Ocean dipole with above normal malaria cases in Vhembe and vice versa. These signals are, however, not as strong as those of the meridional dipole (Fig. 4) in the southwestern Indian Ocean and are further discussed in the following.

Given that the meridional SST dipole pattern in the correlation analysis appears different (marked boxes on Fig. 4) from that of the Indian Ocean subtropical dipole discussed in earlier studies (Behera and Yamagata, 2001; Reason, 2002; Fauchereau et al., 2003; Morioka et al., 2010), a new set of SST indices was defined by taking area averages of the SST anomalies in the boxes east of Madagascar (50–70°E, 30–10°S) and south of Madagascar (30–50°E, 50–30°S) as demarcated in Fig. 4. Consistent with the dipolar correlation pattern, indices from those two poles were in opposite phase throughout the study period (Fig. 7). The index south of Madagascar (hereinafter SM_{SSTA}) became negative around 2006, coinciding the onset of the below normal phase of the malaria incidences (Fig. 2). Although the index east of Madagascar (hereinafter EM_{SSTA}) showed a consistent warming, particularly with positive anomalies since 2000, the anomalies became stronger only around 2005. Therefore, the phase reversal in both poles since 2006 was closely associated with the shift to the below normal phase of malaria prevalence in Vhembe.

The VMI association with both poles of the newly identified southwestern Indian Ocean dipole (viz. EM_{SSTA}, SM_{SSTA}) was further examined to understand the roles of the each pole of the dipole separately. The EM_{SSTA} index had the strongest concurrent correlation

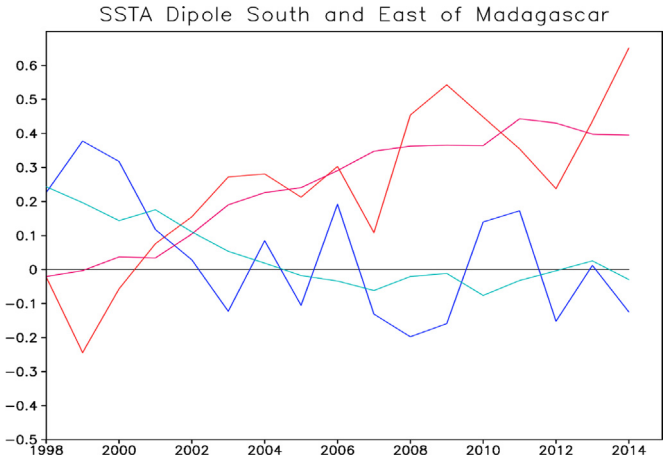

Fig. 7. The time series of seasonal EM_{SSTA} (red) and SM_{SSTA} (blue). High-frequency variations are removed from those two time-series by applying a 13-month running mean. The corresponding time-series of decadal EM_{SSTA} and SM_{SSTA} are shown in magenta and cyan lines. A 7-year running mean is applied to those two time-series to represent the decadal variability (For interpretation of the references to color in this figure legend, the reader is referred to the web version of this article).

with the VMI (−0.73) followed by that of the SM_{SSTA} (0.58) (Table 1). The correlation with EM_{SSTA} got marginally stronger (−0.79) at one season lead, when June-November EM_{SSTA} was correlated with the following September-February VMI. To elucidate the importance of the southwestern Indian Ocean, the VMI was cross-correlated with the indices of other known climate phenomena; namely, Niño3 index for ENSO variability, dipole mode index (DMI) for tropical Indian Ocean dipole variability and Indian Ocean subtropical dipole mode index (IOSDI) for the subtropical dipole variability. At one season lead, the DMI had a significant correlation with VMI though remained lower than that of the EM_{SSTA}. However, the correlations with the Indian Ocean subtropical dipole and ENSO Modoki (values not shown) were not significant.

The above discussed correlations of VMI with other indices remained unaffected when the linear trends were removed from the indices. For example, the correlation for EM_{SSTA} was very slightly decreased (Table 2) but the corresponding correlations for other climate indices did not change that much. This clearly emphasizes the strong impact of the decadal climate trend on long-term decreasing trend of VMI.

Interesting inter-relationships among VMI, EM_{SSTA}, ENSO and IOD were noted (Tables 1 and 2). While the ENSO's relationship with VMI was not significant its relationship with EM_{SSTA} was significant. The ENSO-EM_{SSTA} correlation was stronger when the trends were removed from both time-series (Table 2). This ENSO-EM_{SSTA} relationship is also important for VMI variability since EM_{SSTA} is strongly linked to VMI. The EM_{SSTA} and ENSO link could arise through the atmospheric or oceanic teleconnections. For tracing the oceanic teleconnection, we examined the shedding of oceanic Rossby waves from the coast of Australia. It must be noted that the origin of these Rossby waves is the throughflow waters that pass through the Indonesian throughflow from the Pacific and propagate along the Western coast of Australia. However, examination of the time-longitude plot of sea surface height anomaly did not reveal any such westward wave propagations (Fig. 8) from the Australian coast to the EM_{SSTA} region. Instead, most of the wave propagations to the EM_{SSTA} region were seen to set from the central Indian Ocean west of 70°E. Therefore, it is possible that the ENSO influence was materialized through an atmospheric teleconnection that modulated the subtropical high in the southern Indian Ocean and induced Rossby waves in the interior part of the ocean. The atmospheric teleconnection of ENSO could also take the route of the mid-latitude wave train as discussed in earlier studies.

Most of the variabilities east of Madagascar represented by the EM_{SSTA} is attributable to the southwestern Indian Ocean variability represented by the SM_{SSTA} in the present study. The correlation between them was strong (Table 1) and the historical SST anomalies for those two poles (Fig. 9) further demonstrate the decadal evolution. Both indices were in opposite phases since 1850 except for a period between 1940 and 1970 when that phase difference was not so well-defined.

3.2. The decadal shift in malaria linked to a new climate pattern

A striking phase-shift in the malaria incidence rates was observed after 2006 in the VMI (Fig. 2). Therefore, differences in climate patterns were analyzed (Fig. 10) before and after 2006 in order to understand the decadal climate link to the decadal shift seen in the malaria incidences. The SST anomalies clearly show a switch to a warmer phase east of Madagascar and reduced rainfall over northeastern parts of South Africa (including adjacent regions of Mozambique) after 2006 (Fig. 10). This was associated with moisture divergence over these continental regions and moisture convergence over the warm waters near Madagascar (Fig. 11). The decadal shift in the EM_{SSTA} anomalies was accompanied by a corresponding shift in the SM_{SSTA} anomalies. Although there are some regional rainfall variations on year-to-year times scales, for example slightly above normal rainfall in some parts of South Africa during 2008–2011 period, the decadal rainfall shift over southern Africa in general was seen to be associated with these decadal SST anomalies over southwestern Indian Ocean near Madagascar. Based on observations and the model results, it is noted that these

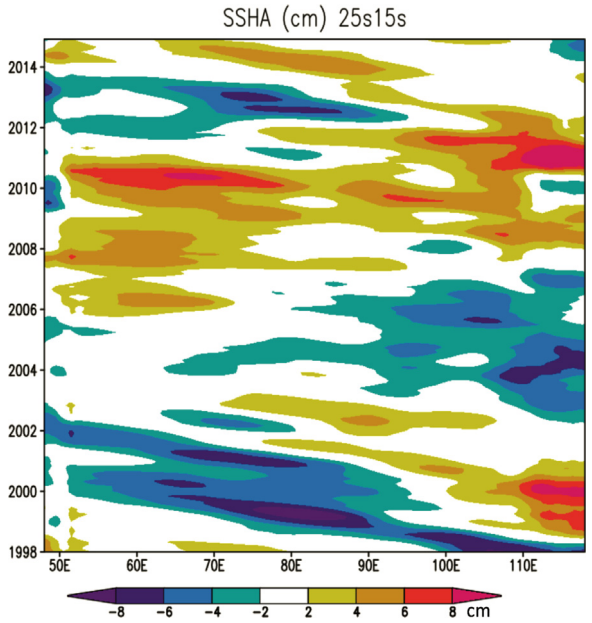

Fig. 8. Longitude-time Hovmöller diagram of SSH anomalies averaged between 25°S and 15°S in the subtropical Indian Ocean. An eleven-month running mean is applied to filter out the high-frequency variations.

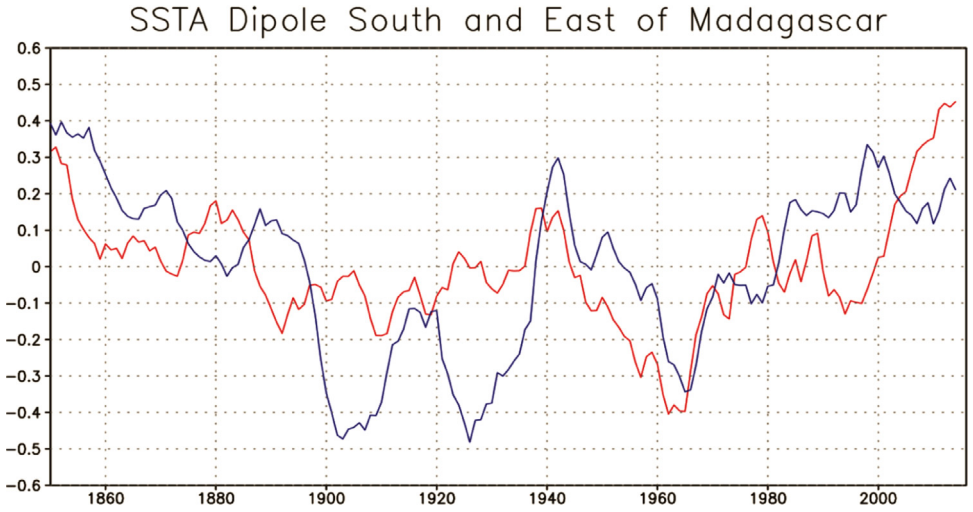

Fig. 9. Time series of decadal EM_{SSTA} and SM_{SSTA} since 1850. The red colored line is for EM_{SSTA} and blue line is for the corresponding SM_{SSTA}. A 7-year running mean is applied to those two time-series to represent the decadal variability (For interpretation of the references to color in this figure legend, the reader is referred to the web version of this article).

anomalies slowly propagate from the South Atlantic to the southwestern Indian Ocean where those get locally coupled with the anomalous lower-tropospheric anticyclone. The stronger/weaker anticyclone associated with the warm/cold phase of the SST anomaly enhanced/reduced the moisture supply to the study region.

In a recent study, Morioka et al. (2015) reported a decadal variability in the southern African rainfall with its positive phase peaking around 1999/2000. These results are consistent with the present finding that the decade prior to 2006 had better rainfall over Vhembe and neighboring regions compared to the decade after 2006. Since the signal was captured by a coupled general circulation model in Morioka et al. study, sensitivity experiments were conducted in their study to understand the underlying processes and triggering mechanisms. It was found that the eastward propagation of the sea level pressure anomaly from the South Atlantic disappears when the SST variability in the South Atlantic was suppressed in the model experiment (Morioka et al., 2015). Nevertheless, it was also found that once placed in the southern Indian Ocean the signal could be sustained through local air-sea interactions.

The Southern Annular Mode or the Antarctic Oscillation (AAO) is often discussed as the other potential source of influence for this

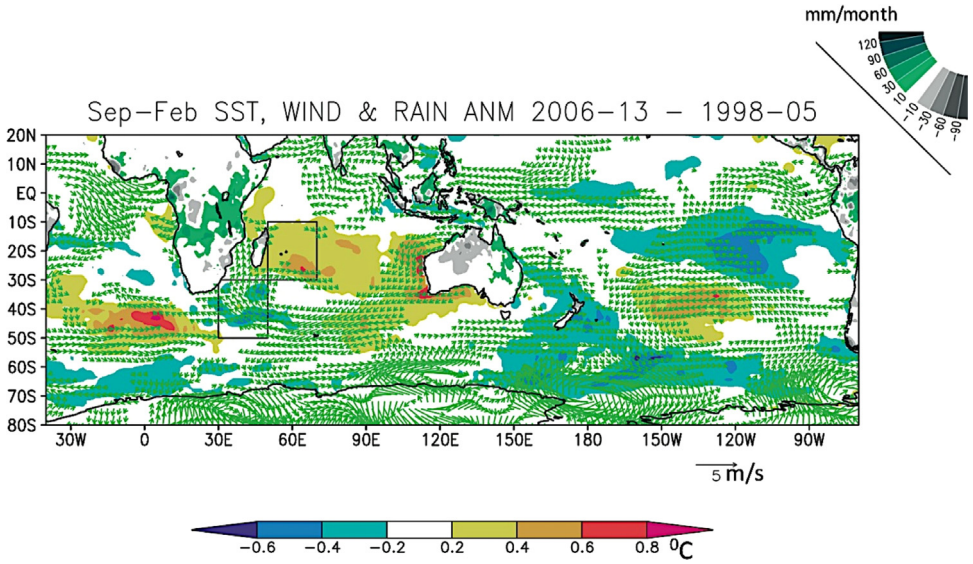

Fig. 10. The differences in SST, rainfall and 850 hPa wind vectors between the two-contrasting period 2006–2013 and 1998–2005 for September–February. SST differences are shaded in the blue to red range and rainfall over land are shaded in the grey to green range (For interpretation of the references to color in this figure legend, the reader is referred to the web version of this article).

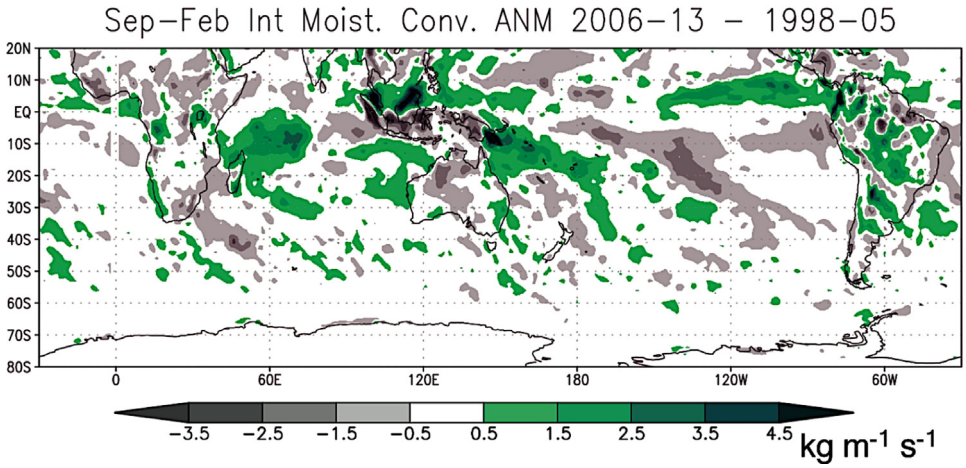

Fig. 11. The differences in moisture flux between the two-contrasting period 2006–2013 and 1998–2005 for September-February. Values are scaled by a factor of 10^5.

region. However, no particular shift was observed in the AAO index between the two-period, around 2006, discussed here thus discounting its role in the phase shift of EM_{SSTA}. Hence, the regional air–sea coupling in southern Indian Ocean as well as South Atlantic is important for the maintenance of the SST anomalies in the southwestern Indian Ocean.

4. Conclusions

A new climate link to variations in malaria incidence of Vhembe district in South Africa is reported here. The climate link was manifested as a dipole pattern in SST anomalies in southwestern Indian Ocean and is different from the tropical and subtropical dipole patterns discussed earlier. The dipole was linked to the malaria incidences in Vhembe district of South Africa with statistically robust relationships.

A decadal shift in the dipole pattern could partly explain malaria remissions during the years after 2006. This downturn in recent years and the associated climate patterns remained unchanged when we replaced the Vhembe index with an averaged malaria incidence index for the top five malaria reporting districts of the Limpopo province, suggesting the robustness of the association. Malaria mosquitoes thrive in the wet and humid climate conditions and anomalously high rainfall would cause mosquito population to explode. But in the last decade, the situation was just opposite. Post 2006, the dipole pattern had shifted to cooler SM_{SSTA} south of Madagascar adjacent to the coasts of southern Africa. This was associated with a weakening of the southwest Indian Ocean

anticyclone, reduced moisture flux to southern Africa and hence less rainfall there on decadal scale. A reduction in the rainfall led to decadal reduction in infection rates explaining below normal malaria prevalence over Vhembe in the recent decade. This shows how climatic factors could influence the long-term variations in malaria incidences in addition to the non-climatic factors (Patz et al., 2005).

The tropical Indian Ocean is warmer in recent years. These warm waters get accumulated east of Madagascar around Mauritius (implicated threat for the sea level rise there) and the basin warming could be a factor contributing to the warming of the EM_{SSTA}. Though the EM_{SSTA} warming trend has continued since 1990s (Fig. 9), it is yet unclear if it will further evolve together with the basin warming trend. Furthermore, as discussed earlier, the southern flank of the dipole pattern (SM_{SSTA}) was apparently triggered by the decadal signal propagating from South Atlantic to southwestern Indian Ocean thereby presenting an extratropical origin of the phenomenon. The southwest Indian Ocean dipole in SST anomalies is therefore linked to tropical as well as extratropical climate variations. This interaction is difficult to capture without a sustained observation program of the southern Indian Ocean, which will greatly help the predictions of the decadal anomalies in southern Indian Ocean and subsequent evolution of SST anomalies. Those in turn will help to develop malaria intervention strategies (Blumberg et al., 2014) for South Africa and adjoining countries. We also note the need to archive records of malaria data to ascertain statistically robust coherence between decadal climate variation and malaria incidences. While we could show just one cycle of the decadal variation in the malaria incidences here, much longer time series of malaria incidence data is needed to understand the long-term fluctuations of malaria cases in relation to low-frequency climate variation.

Acknowledgements

We are thankful to two reviewers for their valuable comments that helped us to improve the quality of the manuscript. We also appreciate the feedbacks from Prof. Angela Mathee, Drs. Patric Moonasar, Jayashree Raman and Caradee Wright. This research was carried out for the iDEWS project supported by SATREPS Program of JICA/AMED in Japan and ACCESS (NRF/DST) in South Africa. An ethical approval to participate in the project is obtained from the Medical Research Council of South Africa. This research is (partially) supported by the Japan Agency for Medical Research and Development, AMED. Analyses were done using GNU Public License software GrADS. Data except for the medical data used in the study are mostly in the public domain and could be made available on request.

References

Behera, S.K., Yamagata, T., 2001. Subtropical SST dipole events in the southern Indian Ocean. Geophys. Res. Lett. 28, 327–330.

Blumberg, et al., 2014. Successfully controlling malaria in South Africa. Malar. Control 104, 224–227.

Chaves, L.F., Satake, A., Hashizume, M., Minakawa, N., 2012. Indian Ocean dipole and rainfall drive a Moran effect in East Africa malaria transmission. J. Infect. Dis. 205, 1885–1891.

Christensen, J.H., Krishna Kumar, K., Aldrian, E., An, S.-.I., Cavalcanti, I.F.A., de Castro, M., Dong, W., Goswami, P., Hall, A., Kanyanga, J.K., Kitoh, A., Kossin, J., Lau, N.-.C., Renwick, J., Stephenson, D.B., Xie, S.-.P., Zhou, T., 2013. Climate Phenomena and their Relevance for Future Regional Climate Change. In: Climate Change 2013: The Physical Science Basis. Contribution of Working Group I to the Fifth Assessment Report of the Intergovernmental Panel on Climate Change [Stocker, T. F., D. Qin, G.-K. Plattner, M. Tignor, S.K. Allen, J. Boschung, A. Nauels, Y. Xia, V. Bex and P.M. Midgley (eds.)]. Cambridge University Press, Cambridge, United Kingdom and New York, NY, USA.

Craig, M.H., Kleinschmidt, I., le Sueur, D., Sharp, B.L., 2004a. Exploring 30 years of malaria case data in KwaZulu-natal, South Africa: Part I. The impact of climatic factors. Trop. Med. Int. Health 9, 1247–1257. http://dx.doi.org/10.1111/j.1365-3156.2004.01340.x.

Craig, M.H., Kleinschmidt, I., le Sueur, D., Sharp, B.L., 2004b. Exploring 30 years of malaria case data in KwaZulu-natal, South Africa: Part II. The impact of non-climatic factors. Trop. Med. Int. Health 2004 9, 1258–1266. http://dx.doi.org/10.1111/j.1365-3156.2004.01341.x.

Fauchereau, N., Trzaska, S., Richard, Y., Roucou, P., Camberlin, P., 2003. Sea-surface temperature co-variability in the Southern Atlantic and Indian Oceans and its connections with the atmospheric circulation in the Southern Hemisphere. Int. J. Clim. 23, 663–677.

Fauchereau, N., Pohl, B., Reason, C., Rouault, M., Richard, Y., 2009. Recurrent daily OLR patterns in the Southern Africa/Southwest Indian Ocean region, implications for South African rainfall and teleconnections. Clim. Dyn. 32, 575–591.

Gerritsen, A.M.A., Kruger, P., Schim van der Loeff, M.F., Grobusch, M.P., 2008. Malaria incidence in Limpopo Province, South Africa, 1998–2007. Malar. J. 7, 162. http://dx.doi.org/10.1186/1475-2875-7-162.

Giannini, A., Biasutti, M., Held, I., Sobel, A., 2008. A global perspective on African climate. Clim. Change 90, 359–383.

Hansingo, K., Reason, C.J.C., 2008. Modelling the atmospheric response to SST dipole patterns in the South Indian Ocean with a regional climate model. Meteorol. Atmos. Phys. 100, 37–52.

Hansingo, K., Reason, C.J.C., 2009. Modelling the atmospheric response over southern Africa to SST forcing in the southeast tropical Atlantic and southwest sub-tropical Indian Oceans. Int. J. Climatol. 29, 1001–1012. http://dx.doi.org/10.1002/joc.1919.

Hashizume, M., Terao, T., Minakawa, N., 2009. The Indian Ocean Dipole and malaria risk in the highlands of western Kenya. Proc. Natl. Acad. Sci. USA 106, 1857–1862.

Hashizume, M., Chaves, L.F., Minakawa, N., 2012. Indian ocean dipole drives malaria resurgence in East African highlands. Sci. Rep. 2, 1–6.

Hermes, J.C., Reason, C.J.C., 2008. Annual cycle of the south Indian Ocean (Sey-chelles-Chagos) thermocline ridge in a regional ocean model. J. Geophys. Res. 113 (C04), 035.

Ikeda T et al., (2017), Seasonally lagged effects of climatic factors on malaria incidence in South Africa, 7(1): 2458. 〈http://www.nature.com/articles/s41598-017-02680-6〉.

Ishii, M., Shouji, A., Sugimoto, S., Matsumoto, T., 2005. Objective analyses of sea-surface temperature and marine meteorological variables for the 20th century using ICOADS and the Kobe collection. Int. J. Climatol. 25, 865–879.

Japan Meteorological Agency, 2006. Characteristics of global sea surface temperature analysis data (COBE-SST) for climate use. Mon. Report. Clim. Syst. Sep. Vol. 12 (116pp).

Jury, M., Kanemba, A.A., 2007. climate-based model for malaria prediction in southeastern Africa. S. Afr. J. Sci. 103, 57–62.

Kanamitsu, et al., 2002. NCEP–DOE AMIP-II Reanalysis (R-2). Bull. Am. Met. Soc. 83, 1631–1643.

Kirtman, B., Power, S.B., Adedoyin, J.A., Boer, G.J., Bojariu, R., Camilloni, I., Doblas-Reyes, F.J., Fiore, A.M., Kimoto, M., Meehl, G.A., Prather, M., Sarr, A., Schär, C., Sutton, R., van Oldenborgh, G.J., Vecchi, G., Wang, H.J., 2013. Near-term climate change: projections and predictability. In: Stocker, T.F., Qin, D., Plattner, G.-K., Tignor, M., Allen, S.K., Boschung, J., Nauels, A., Xia, Y., Bex, V., Midgley, P.M. (Eds.), Climate Change 2013: The Physical Science Basis. Contribution of Working

Group I to the Fifth Assessment Report of the Intergovernmental Panel on Climate Change. Cambridge University Press, Cambridge, United Kingdom and New York, NY, USA.
Mabaso, M.L., Kleinschmidt, I., Sharp, B., Smith, T., 2007. El Nino Southern Oscillation (ENSO) and annual malaria incidence in Southern Africa. Trans. R. Soc. Trop. Med Hyg. 101 (4), 326–330.
Maharaj, R., Morris, N., Seocharan, I., Kruger, P., Moonasar, D., Mabuza, A., Raswiswi, E., Raman, J., 2012. The feasibility of malaria elimination in South Africa. Malar. J. 11, 423. http://dx.doi.org/10.1186/1475-2875-11-423.
Maharaj, R., Raman, J., Morris, N., Moonasar, D., Durrheim, D.N., Seocharan, I., Kruger, P., Shandukani, B., Kleinschmidt, I., 2013. Epidemiology of malaria in South Africa: from control to elimination. Epidemiology 103, 779–783.
Manatsa, D., Chingombe, W., Matsikwa, H., Matarira, C.H., 2008. The superior influence of Darwin Sea level pressure anomalies over ENSO as a simple drought predictor for Southern Africa. Theor. Appl. Climatol. 92, 1–14.
Mason, S., 2001. El Nino, climate change, and Southern African climate. Environmetrics 12, 327–345.
Moonasar, et al., 2012. Malaria control in South Africa 2000–2010: beyond MDG6. Malar. J. 11, 294.
Morioka, Y., Tozuka, T., Yamagata, T., 2010. Climate variability in the southern Indian Ocean as revealed by self-organizing maps. Clim. Dyn. 35, 1075–1088.
Morioka, Y., Engelbrecht, F., Behera, S.K., 2015. Potential sources of decadal climate variability over southern Africa. J. Clim. 28, 8695–8709 (doi: 0.1175/JCLI-d-14-00133.1).
Patz, A.J., Lendrum, D.C., Holloway, T., Foley, J.A., 2005. Impact of regional climate change on human health. Nature 438, 310–317. http://dx.doi.org/10.1038/nature04188.
Pohl, B., Fauchereau, N., Reason, C., Rouault, M., 2010. Relationships between the Antarctic oscillation, the Madden - Julian oscillation, and ENSO, and consequences for rainfall analysis. J. Clim. 23, 238–254.
Raman, J., Morris, N., Frean, J., Brooke, B., Blumberg, L., Kruger, P., Mabusa, A., Raswiswi, E., Shandukani, B., Misani, E., Groepe, M.-A., Moonasar, D., 2016. Reviewing South Africa's malaria elimination strategy (2012–2018): progress, challenges and priorities. Malar. J. 15, 438.
Reason, C.J.C., 2002. Sensitivity of the southern African circulation to dipole sea-surface temperature patterns in the south Indian Ocean. Int. J. Climatol. 22, 377–393. http://dx.doi.org/10.1002/joc.744.
Reynolds, et al., 2002. An improved in situ and satellite SST analysis for climate. J. Clim. 15, 1609–1625.
Rouault, M., Florenchie, P., Fauchereau, N., Reason, C.J.C., 2003. Southeast tropical Atlantic warm events and southern African rainfall. Geo- phys. Res. Lett. 30, 8009. http://dx.doi.org/10.1029/2002GL014840.
Schneider, et al., 2013. GPCC's new land surface precipitation climatology based on quality-controlled in situ data and its role in quantifying the global water cycle. Theo. Appl. Climatol. 115, 15–40. http://dx.doi.org/10.1007/s00704-013-0860-x.
Vigaud, N., Richard, Y., Rouault, M., Fauchereau, N., 2009. Moisture transport between the South Atlantic Ocean and southern Africa: relationships with summer rainfall and associated dynamics. Clim. Dyn. 32, 113–123.